

See discussions, stats, and author profiles for this publication at: <https://www.researchgate.net/publication/264202408>

# Third-Order Nonlinear Optical Properties of One-Dimensional Open-Shell Molecular Aggregates Composed of Phenalenyl Radicals

ARTICLE *in* CHEMISTRY - A EUROPEAN JOURNAL · AUGUST 2014

Impact Factor: 5.73 · DOI: 10.1002/chem.201402197 · Source: PubMed

CITATIONS

5

READS

57

9 AUTHORS, INCLUDING:



**Kyohei Yoneda**

Nara National College of Technology

42 PUBLICATIONS 592 CITATIONS

SEE PROFILE



**Masayoshi Nakano**

Osaka University

334 PUBLICATIONS 4,714 CITATIONS

SEE PROFILE



**Takashi Kubo**

Osaka University

136 PUBLICATIONS 2,948 CITATIONS

SEE PROFILE



**Benoît Champagne**

University of Namur

400 PUBLICATIONS 8,600 CITATIONS

SEE PROFILE

## ■ Nonlinear Optics

## Third-Order Nonlinear Optical Properties of One-Dimensional Open-Shell Molecular Aggregates Composed of Phenalenyl Radicals

Kyohei Yoneda,<sup>[a]</sup> Masayoshi Nakano,<sup>\*[a]</sup> Kotaro Fukuda,<sup>[a]</sup> Hiroshi Matsui,<sup>[a]</sup> Shota Takamuku,<sup>[a]</sup> Yuta Hirosaki,<sup>[a]</sup> Takashi Kubo,<sup>[b]</sup> Kenji Kamada,<sup>[c]</sup> and Benoît Champagne<sup>[d]</sup>

**Abstract:** The impact of intermolecular interactions on the third-order nonlinear optical (NLO) properties of open-shell molecular aggregates has been elucidated by considering one-dimensional aggregates of  $\pi$ - $\pi$  stacked phenalenyl radicals with different intermolecular distances and the long-range corrected spin-unrestricted density functional theory method. In the phenalenyl dimer, which can be considered as a diradicaloid system, the diradical character strongly depends on the intermolecular distance, and the larger the intermolecular distance is, the larger the diradical character becomes. Then, around the equilibrium stacking distance that corresponds to an intermediate diradical character, its second hyperpolarizability ( $\gamma$ ) is maximized and its value per monomer exhibits about a 30-fold enhancement with respect to the isolated phenalenyl monomer. This suggests

that equilibrium is an optimal compromise between localization and delocalization of the radical electron pairs in such pancake bonding. No such effect was observed for the closed-shell coronene dimer. Moreover, when going from the dimer (diradical) to the tetramer (tetraradical), the  $\gamma$ -enhancement ratio increases nonlinearly with the aggregate size, whereas switching from the singlet to the highest spin (quintet) state causes a significant reduction of  $\gamma$ . Finally, for the tetramer, another one-order enhancement of  $\gamma$  is achieved for the dicationic singlet relative to its singlet neutral state. These results demonstrate the key role of intermolecular  $\pi$ - $\pi$  stacking interactions and charge in open-shell (supra)molecular systems to achieve enhanced third-order NLO properties.

## Introduction

Compounds with highly efficient nonlinear optical (NLO) properties have been expected to be fundamental substances for future photonics applications, such as ultrafast optical switching,<sup>[1a]</sup> high-capacity three-dimensional memory,<sup>[1b]</sup> three-di-

mensional microfabrication,<sup>[1c,d]</sup> efficient optical limiting,<sup>[1e]</sup> and photodynamic therapy.<sup>[1f]</sup> On the basis of the experimental and theoretical studies, structure/NLO-property relationships have been deduced for several tuning parameters (e.g., the structure and size of  $\pi$ -conjugated linkers, and the strength of donor/acceptor substituents). However, most studies on the design and realization of highly efficient NLO materials have concentrated on closed-shell systems. Recently, we have proposed open-shell singlet molecular systems as a novel class of NLO substances on the basis of theoretical and computational studies.<sup>[2]</sup> The electronic structure of these open-shell singlets is characterized by the diradical character ( $y$ ) (0 (closed-shell system)  $\leq y \leq 1$  (pure open-shell system)), which is well defined in quantum chemistry,<sup>[3]</sup> whereas  $1-y$  corresponds to an effective chemical bond order between the two radicals.<sup>[3b]</sup> It has been evidenced that the second hyperpolarizability ( $\gamma$ )—the molecular property at the source of the third-order NLO properties—exhibits a remarkable dependence on the diradical character ( $y$ ): systems with intermediate  $y$  values tend to exhibit a large enhancement of  $\gamma$  relative to the closed-shell and pure diradical systems of similar molecular sizes.<sup>[2,4,5]</sup> The mechanism of this enhancement has been clarified using analytical expressions derived from the valence configuration interaction (VCI) theory based on a two-site model with two

[a] K. Yoneda, Prof. Dr. M. Nakano, K. Fukuda, H. Matsui, S. Takamuku, Y. Hirosaki  
Department of Materials Engineering Science  
Graduate School of Engineering Science, Osaka University  
Toyonaka, Osaka 560-8531 (Japan)  
Fax: (+81)6-6850-6268  
E-mail: mnaka@cheng.es.osaka-u.ac.jp

[b] Prof. Dr. T. Kubo  
Department of Chemistry, Graduate School of Science  
Osaka University, Toyonaka, Osaka 560-0043 (Japan)

[c] Dr. K. Kamada  
Research Institute for Ubiquitous Energy Devices  
National Institute of Advanced Industrial Science and Technology (AIST), Ikeda, Osaka 563-8577 (Japan)

[d] Prof. Dr. B. Champagne  
Laboratoire de Chimie Théorique (LCT)  
University of Namur, Rue de Bruxelles, 61  
5000 Namur, Belgium (Belgium)

Supporting information for this article is available on the WWW under <http://dx.doi.org/10.1002/chem.201402197>.

electrons in two magnetic orbitals.<sup>[6]</sup> This analysis has also been exemplified using highly accurate ab initio molecular orbital (MO) and spin-unrestricted density functional theory (UDFT) calculations for various model and real open-shell molecular systems, including *p*-quinodimethane,<sup>[2a]</sup> imidazole and triazole benzenes,<sup>[2b]</sup> H<sub>2</sub> molecules in the dissociation process,<sup>[2c]</sup> polycyclic hydrocarbons,<sup>[2d,4]</sup> multinuclear transition-metal complexes,<sup>[5]</sup> and thiophene-based systems.<sup>[2e]</sup> Subsequently, this diradical character dependence of  $\gamma$  has been confirmed experimentally by remarkably large two-photon absorption cross-sections (a typical third-order NLO property) of several polycyclic aromatic diphenalenyl diradicaloids,<sup>[7,8]</sup> which are thermally stable diradical systems and are predicted to possess intermediate  $\gamma$  values. Furthermore, we have also reported the relationship between the NLO properties and multiradical character using several one-dimensional (1D) multiradical systems, including the hydrogen-atom chain models.<sup>[9]</sup> It has been revealed that the  $\gamma$  values of the intermediate 1D multiradical systems exhibit significantly enhanced amplitudes relative to those of the closed-shell and pure multiradical counterparts, and also show significant chain-length dependences comparable to those of closed-shell counterparts.

As a real system for the above 1D chain model, we have theoretically found that for *s*-indaceno[1,2,3*cd*:5,6,7-*c'd'*]diphenylene (IDPL), which is a typical diphenalenyl diradicaloid, the dimerization significantly enhances the  $\gamma$  value per monomer relative to that of the isolated monomer, the feature of which is caused by the emergence of a tetraradical nature owing to the covalent-like intermolecular interaction through their radical sites.<sup>[10]</sup> This theoretical prediction corresponds well with the experimental results<sup>[7a]</sup> that the IDPL crystal, composed of 1D molecular chains with a slipped stacking arrangement, displays an unusually short average  $\pi$ - $\pi$  distance (3.137 Å), which is less than the sum of the van der Waals radius (3.4 Å), and causes an energy shift to an extraordinary lower-frequency region in the optical spectrum than that of the monomers in solution (i.e., from 746 nm in solution in dichloromethane to 1670 nm in the crystal). These results indicate that extended multiradical structures exist in real solid crystals composed of open-shell molecules, and that they will contribute to achieving novel design strategies of open-shell NLO materials by tuning the multiradical character through controlling the intermolecular interactions.

By using first-principles methods, the aim of the present study is to elucidate the role of intermolecular interactions in open-shell aggregates on their open-shell character and NLO properties. These molecular aggregates are composed of  $\pi$ - $\pi$  stacked phenalenyl radicals with different intermolecular distances. As with IDPL, the presence of covalent-like intermolecular interactions has also been suggested for the phenalenyl dimer in a number of experimental<sup>[11]</sup> and theoretical studies.<sup>[12,13]</sup> For example, Zhong et al. have theoretically investigated the dimers of phenalenyl families and predicted that the hexaazaphenalenyl dimer possesses an intermediate diradical character and a large  $\gamma$  value,<sup>[13]</sup> but the intermolecular distance dependence on  $\gamma$  and  $\gamma$  has not been clarified. First, we investigate the phenalenyl dimers, which are considered sin-

glet diradical systems, in comparison to coronene dimers, which are considered reference closed-shell systems. Then, we examine the tetramers to reveal the multiradical effects on the  $\gamma$  values in the stacking direction. Furthermore, the charge and spin-state dependences of the  $\gamma$  values of these multiradical systems are studied from the viewpoint of additional tuning parameters. These calculations are carried out using density functional theory (DFT) and in particular the long-range corrected UDFT (i.e., LC-UBLYP) method.<sup>[14]</sup> The present study contributes to the understanding of the multiradical characters induced in open-shell molecular aggregates and/or open-shell solids, and thus to the elaboration of novel guidelines for designing highly efficient third-order NLO materials based on the multiradical molecular aggregates.

## Computational Methods

### Structures of model systems

Figure 1 shows the molecular structures of the phenalenyl radical (a) with *D*<sub>3h</sub> symmetry optimized using the UB3LYP/6-31G\* method, and of two types of  $\pi$ - $\pi$  dimers (i.e., the eclipsed- (b) and anti- (or staggered) (c) types). The calculations for the phenalenyl

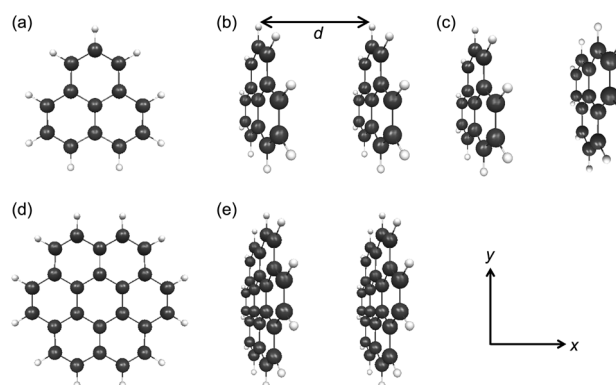


**Figure 1.** Molecular structures of the a) phenalenyl radical, b) eclipsed-type and c) anti-type phenalenyl dimers, as well as d) coronene and e) its dimer. Carbon and hydrogen atoms are represented by dark and white circles, respectively.

aggregates (for any intermolecular stacking distance *d*) were carried out using  $\pi$ - $\pi$  stacked monomers, with geometries frozen to those of the optimized isolated monomer. For the two types of dimers, we examined the binding energy as a function of *d* in the range from 2.8 to 6.0 Å by using the UB3LYP XC functional augmented with Grimme's D2 empirical dispersion term (UB3LYP-D)<sup>[15]</sup> together with the 6-31+G\* basis set. Additional calculations were also performed using the UM06-2X and  $\omega$ UB97X-D XC functionals. We also applied the counterpoise correction for the basis set superposition error (BSSE).<sup>[16]</sup> The structures of closed-shell coronene, optimized using the UB3LYP/6-31G\* method, and those of the dimer built from the optimized monomer geometries, in which the monomers fully eclipse each other, are also displayed in Figure 1d and e, respectively.

## Open-shell character

The electronic structure of multiradical systems is characterized by multiple diradical characters  $y_i$ , which represent the instability of chemical bonds between radical pairs.<sup>[3,17,18]</sup> For single-determinant schemes, the diradical character  $y_i$  (related to the highest- $i$  occupied natural orbital (HONO- $i$ ) and the lowest- $i$  unoccupied natural orbital (LUNO- $i$ )) is defined by the occupation number ( $n_k$ ) of the corresponding natural orbitals (NOs) [Eq. (1)]:

$$y_i = n_{\text{LUNO}+i} = 2 - n_{\text{HONO}-i} \quad (1)$$

which takes a value that ranges from 0 (closed-shell) to 1 (pure diradical). The  $y_i$  values were calculated using the LC-UBLYP with  $\mu = 0.33$  and the 6-31+G\* basis set. They were not corrected for spin contamination by projection, unlike the  $y_i$  obtained from the UHF NO (UNO) occupation numbers,<sup>[2]</sup> because the spin contamination effect is generally smaller when using UDFt than the UHF method. The spatial contributions to the open-shell natures are described by analyzing the odd-electron density,<sup>[3d,18]</sup>  $D^{\text{odd}}(\mathbf{r})$ , defined from the NOs  $\varphi_k(\mathbf{r})$  and their occupation numbers  $n_k$  [Eq. (2)].<sup>[18]</sup>

$$D^{\text{odd}}(\mathbf{r}) = \sum_k \min(2 - n_k, n_k) \varphi_k^*(\mathbf{r}) \varphi_k(\mathbf{r}), \quad (2)$$

in which the  $\min(2 - n_k, n_k)$  factor can be regarded as the probability for the electron of being unpaired in  $\varphi_k(\mathbf{r})$ .

## Second hyperpolarizability

The  $\gamma$  calculations were also performed at the LC-UBLYP/6-31+G\* level because it has been found to semiquantitatively reproduce the second hyperpolarizabilities of several diradical molecules calculated using strongly correlated post-unrestricted Hartree-Fock (post-UHF) methods (e.g., the spin-unrestricted coupled-cluster method including single and double excitations with a perturbative treatment of the triple excitations (UCCSD(T))).<sup>[19]</sup> Only the diagonal tensor component of  $\gamma$  along  $x$  ( $\gamma_{xxxx}$ ) was evaluated, in which the  $x$  axis indicates the  $\pi$ - $\pi$  stacking direction. Indeed, the  $\gamma$  enhancement effect due to intermediate open-shell character appears only for the component along the line that connects the two radical sites. The  $\gamma_{xxxx}$  values were calculated using the finite-field approach,<sup>[20]</sup> which consists in the fourth-order numerical differentiation of the energy with respect to the applied external electric field. The field amplitudes were chosen so as to achieve a numerical accuracy within an error of 1% on the  $\gamma_{xxxx}$  value. The  $\gamma_{xxxx}$  values were corrected for BSSE by the counterpoise scheme, but these corrections are negligibly small (less than 1% of the total  $\gamma_{xxxx}$  value) for most of the cases (see the Supporting Information for details). The perturbation series expansion convention, which is usually called the B convention, was employed for the definition of  $\gamma_{xxxx}$ .

The spatial contributions of the electrons to  $\gamma_{xxxx}$  were scrutinized by analyzing the  $\gamma$  density,<sup>[21]</sup>  $\rho_{xxx}^{(3)}(\mathbf{r})$ , which was numerically calculated as the third derivative of electron density with respect to the applied electric field [Eq. (3)]:

$$\rho_{xxx}^{(3)}(\mathbf{r}) = \frac{\partial^3 \rho}{\partial F_x \partial F_x \partial F_x} \Big|_{F=0} \quad (3)$$

Using this density,  $\gamma_{xxxx}$  was obtained by Equation (4):

$$\gamma_{xxxx} = -\frac{1}{3!} \int r_x \rho_{xxx}^{(3)}(\mathbf{r}) d^3 \mathbf{r} \quad (4)$$

A pair of positive and negative  $\rho_{xxx}^{(3)}(\mathbf{r})$  distributions placed consecutively along the  $x$  axis gives rise to a positive  $\gamma_{xxxx}$  contribution, which is proportional to the product of the density amplitude and the pair distance. In the following sections,  $\gamma_{xxxx}$  and  $\rho_{xxx}^{(3)}(\mathbf{r})$  are referred to as  $\gamma$  and  $\rho^{(3)}(\mathbf{r})$ , respectively. All calculations were performed using the Gaussian 09 program package.<sup>[22]</sup>

## Results and Discussion

### Dimers

Before investigating the dimers, the adequacy of the 6-31+G\* basis set was addressed by examining  $\gamma$  of the phenalenyl monomer. The  $\gamma$  values calculated using the selected basis set reproduced within 0.7% those obtained using the much extended and reference aug-cc-pVTZ basis set (Table 1). This confirms the need for diffuse functions for quantitative estimations of  $\gamma$  of phenalenyl.

**Table 1.** Out-of-plane diagonal components of  $\gamma$  ( $\gamma_{xxxx}$ ) for the phenalenyl radical monomer calculated using the LC-UBLYP method with several basis sets.

Basis set	$\gamma$ [a.u.]
6-31G*	8
6-31+G*	2980
6-311++G**	3150
aug-cc-pVTZ	3000

Figure 2a shows the potential-energy curves [ $E(\text{dimer}) - 2E(\text{monomer})$ ] for the eclipsed and anti-type phenalenyl dimers as a function of the stacking distance  $d$  calculated using the UB3LYP-D/6-31+G\* method. The equilibrium distances are  $d = 3.3$  and  $3.0$  Å for the eclipsed and anti types, respectively, both of which are shorter than twice the van der Waals radius of the carbon atom ( $2 \times 1.7$  Å =  $3.4$  Å). The binding energies of the eclipsed and anti dimers are  $9.4$  and  $17.9$  kcal mol<sup>-1</sup> ( $8.2$  and  $15.6$  kcal mol<sup>-1</sup> upon including the zero-point vibrational corrections), respectively (i.e., the anti-stacking structure is the most stable). The equilibrium stacking distance and the binding energies of the anti dimer are found to be consistent with earlier results by Zhong et al.,<sup>[13]</sup> although they employed different functionals as well as slightly different monomer geometries ( $d = 3.1$  Å, bonding energy =  $16.82$  kcal mol<sup>-1</sup> (M06-2X)). It has been reported from X-ray analysis that, in the crystal phase, the 2,5,8-tri-*tert*-butylphenalenyl compound displays anti-type  $\pi$ - $\pi$  stacking structure,<sup>[11]</sup> which is in good agreement with our predictions. However, the experimental stacking distance in the crystal is  $3.2$  Å, in comparison to  $3.0$  Å for the dimer, the difference being attributed to crystal packing and substituents effects. In addition, the binding energies (enthal-

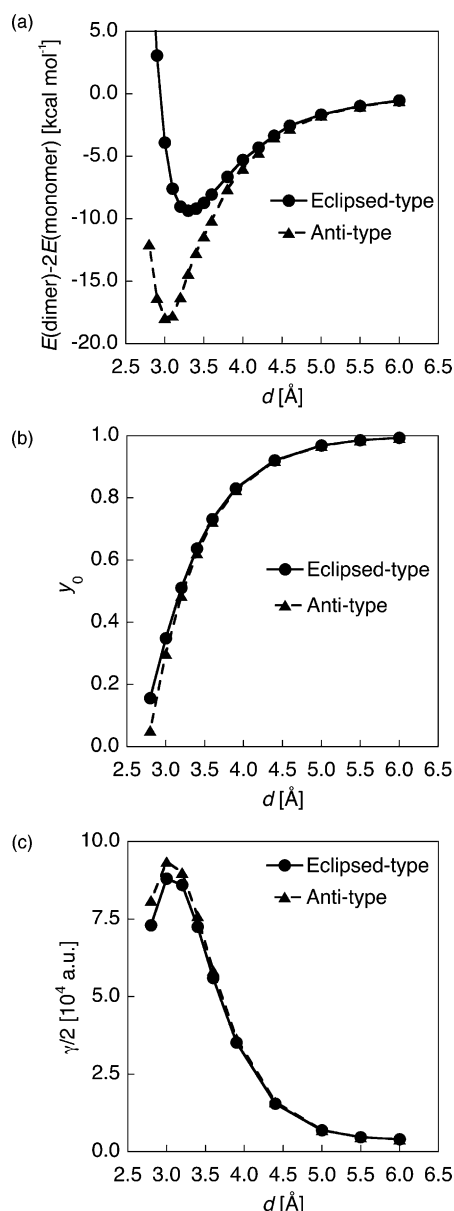


**Figure 2.** Potential-energy curves ( $E(\text{dimer}) - 2E(\text{monomer})$ ) a) calculated using the UB3LYP-D/6-31+G\* method, b) diradical characters  $y_0$ , and c)  $\gamma/2$  values calculated using the LC-UBLYP/6-31+G\* method as a function of stacking distance  $d$  for the eclipsed and anti-phenalenyl dimers.

pies) for solutions of the dimer of 2,5,8-tri-*tert*-butylphenalenyl in hexane and dichloromethane amount to 7.5 and 9.5 kcal mol<sup>-1</sup>, respectively,<sup>[23]</sup> which indicates that the UB3LYP-D method exhibits an overbinding in the  $\pi$ - $\pi$  stacking of the phenalenyl dimer. In the present case, the solvent effects are not considered, because they are expected to be small in these systems with covalent-like intermolecular interactions and no donor-acceptor substituents. These results were substantiated by using other XC functionals, UM06-2X and  $\omega$ UB97X-D, which give the potential-energy curves shown in Figure S1 of the Supporting Information. Although these functionals provide better stacking distances and interaction energies (3.1 Å and 13.4 kcal mol<sup>-1</sup> at UM06-2X and 3.2 Å and

12.2 kcal mol<sup>-1</sup> at  $\omega$ UB97X-D) than UB3LYP-D, part of the over-binding tendency remains. Note also that Kolb et al. investigated the binding interactions in the phenalenyl dimer by using the multireference perturbation theory, CASSCF(2,2)-MP2, method and the van der Waals density functional (vdW-DF) method and that both methods also significantly overestimate the binding energy [30.9 kcal mol<sup>-1</sup> (CASSCF-MP2) and 14.6 kcal mol<sup>-1</sup> (vdW-DF)].<sup>[12b]</sup> Considering these results, we conclude that the stable structure of the phenalenyl dimer adopts an anti-stacking configuration with a stacking distance smaller than the usual van der Waals distance, although a quantitative prediction of the binding energy is an open question.

The  $d$  dependences of the diradical character ( $y_0$ ) for the two types of phenalenyl dimers are shown in Figure 2b (see also Table S1 in the Supporting Information). The  $y_i$  ( $i \geq 1$ ) values are negligibly small (e.g.,  $0.018 \leq y_1 \leq 0.022$  at  $2.8 \text{ Å} \leq d \leq 6.0 \text{ Å}$  for the eclipsed dimer), which means that the phenalenyl dimers are regarded as diradical or diradicaloid systems. There is little difference in  $y_0$  values between the eclipsed and anti dimers, which both exhibit a wide range of diradical characters from nearly closed-shell to pure diradical state as a function of the stacking distance. This involves the existence of strong covalent-like intermolecular interactions at short  $d$ .<sup>[12,13]</sup> Then, for  $d = 3.2 \text{ Å}$ , which is equal to the experimental stacking distance in the crystal structure, the systems show an intermediate  $y_0$  value [ $y_0 = 0.511$  (eclipsed) and 0.485 (anti)], which corresponds to weak covalent bonds between the radicals. The fact that the intermediate diradical character emerges around the equilibrium stacking distance in the phenalenyl radical dimer suggests an optimum compromise between localization and delocalization of the radical electron pairs in such pancake bonding. Figure 3 shows  $D^{\text{odd}}(r)$  for a) the phenalenyl monomer and b) the anti dimers with  $d = 3.0 \text{ Å}$  and c)  $6.0 \text{ Å}$ . The shape of  $D^{\text{odd}}(r)$  is very similar for both the dimers and the monomer, whereas the amplitudes are different, which is directly correlated to the amplitudes of their diradical characters. In the case of  $d = 3.0 \text{ Å}$ , which leads to an intermediate diradical system ( $y_0 = 0.299$ ), the  $D^{\text{odd}}(r)$  amplitude is reduced relative to the isolated monomer. In contrast, for the dimer with  $d = 6.0 \text{ Å}$ , which is nearly a pure diradical ( $y_0 = 0.993$ ), it hardly changes from that of the monomer and is thus much larger than that of the dimer with  $d = 3.0 \text{ Å}$ .

The evolution of  $\gamma$  per monomer (i.e.,  $\gamma/2$ ) calculated using the LC-UBLYP/6-31+G\* method as a function of the stacking distances is similar for both dimers (Figure 2c). The phenalenyl dimers show a significant  $\gamma$  enhancement in the intermediate diradical region (Figure 2b), which coincides with the diradical character dependence of  $\gamma$  for single diradical molecules observed in previous studies.<sup>[2]</sup> In particular, the  $\gamma$  values per monomer [ $\gamma/2 = 8.75 \times 10^4$  a.u. (eclipsed) and  $9.30 \times 10^4$  a.u. (anti)] of the dimers at  $d = 3.0 \text{ Å}$  that correspond to intermediate  $y_0$  [0.348 (eclipsed) and 0.299 (anti)] are about 30 times as large as that of the isolated monomer ( $\gamma = 2980$  a.u.), whereas for  $d = 6.0 \text{ Å}$  ( $\gamma/2 = 0.39 \times 10^4$  a.u. for both types), the increase ratio attains only 30%.

Next, to clarify the relationship between the open-shell characters and  $\gamma$  values, the spatial electronic contributions to  $\gamma$



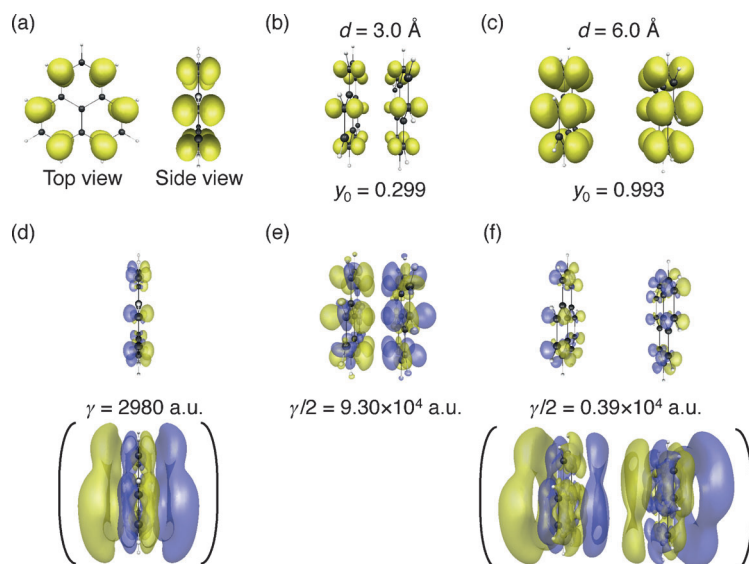


**Figure 3.** Odd-electron density ( $D^{\text{odd}}(r)$ ) distributions for a) phenalenyl monomer and b) the anti dimers with  $d = 3.0$  Å and c)  $6.0$  Å, as well as their  $y_0$  values, in which the iso-surfaces of  $0.002$  a.u. are shown. d–f) The  $\gamma$  density ( $\rho^{(3)}(r)$ ) distributions and  $\gamma$  per monomer for the same systems are also shown. The yellow and blue meshes represent positive and negative distributions with isosurfaces of  $\pm 10$  a.u. for the monomer and dimer with  $d = 6.0$  Å and of  $\pm 600$  a.u. for the dimer with  $d = 3.0$  Å. In parentheses,  $\rho^{(3)}(r)$  distributions for (d) and (f) are also shown with isosurfaces of  $\pm 3$  a.u.

were analyzed using  $\rho^{(3)}(r)$ . The  $\rho^{(3)}(r)$  distributions for the phenalenyl monomer and anti dimers with  $d = 3.0$  and  $6.0$  Å are shown in Figure 3d,e, and f, respectively. The relationship among these  $\rho^{(3)}(r)$  amplitudes clearly substantiates the difference in their  $\gamma$  values: 1) the  $\rho^{(3)}(r)$  distribution of the dimer with  $d = 6.0$  Å shows little difference from that of the monomer, and 2) for  $d = 3.0$  Å, it is significantly larger and shows a completely different  $\rho^{(3)}(r)$  distribution, which is dominated by the field-induced  $\pi$ -electron transfer between the monomers. These  $\rho^{(3)}(r)$  distributions are very similar to the odd-electron distributions (see Figure 3b and c), which substantiates the intermediate diradical character origin of the  $\gamma$  enhancement.

The impact of structural relaxation effects was then assessed by calculating  $y$  and  $\gamma/2$ —at the LC-UBLYP/6-31G\* level—for the anti dimer, the structure of which was optimized at the UB3LYP-D/6-31G\* level under the constraint of imposing the stacking distance (central C–C distance) to  $3.0$  Å. The value of  $y$  slightly decreases ( $y_0 = 0.260$ ) relative to that of the unrelaxed dimer ( $y_0 = 0.299$ ), whereas  $\gamma$  shows no change (i.e.,  $\gamma/2 = 9.30 \times 10^4$  a.u.). Furthermore, we characterize with the LC-UBLYP/6-31+G\* method the structures optimized by using the UM06-2X and  $\omega$ UB97X-D methods for a fixed stacking distance  $d = 3.0$  Å. Although slight changes in  $y_0$  values are observed ( $y_0 = 0.294$  (UM06-2X) and  $0.384$  ( $\omega$ UB97X-D)), the changes in  $\gamma/2$  values are less than 1% of the  $\gamma/2$  ( $\gamma/2 = 9.45 \times 10^4$  a.u. (UM06-2X) and  $9.35 \times 10^4$  a.u. ( $\omega$ UB97X-D)), which indicates that the structural relaxation effects are negligible on the  $\gamma$  value of the phenalenyl dimer.

The coronene dimer, which is a closed-shell analogue, was then examined. LC-RBLYP/6-31+G\*  $\gamma/2$  values calculated for

different stacking distances (Figure 4 and Table S2 in the Supporting Information) demonstrate that  $\gamma$  of the coronene dimer remains mostly constant, unlike for the phenalenyl dimer, and that  $\gamma/2$  of the dimer is very close to  $\gamma$  of the monomer ( $4010$  a.u.). Although isolated coronene exhibits a larger  $\gamma$  value than phenalenyl, the relative  $\gamma$  values of the dimers are inverted, provided the diradical character is intermediate; e.g.,  $\gamma/2 = 9.30 \times 10^4$  a.u. (anti-phenalenyl dimer) versus  $0.52 \times 10^4$  a.u. (coronene) at  $d = 3.0$  Å.

## Tetramers

Since the stacking type has almost no impact on  $y$  and  $\gamma$  of the phenalenyl dimers, only phenalenyl tetramers with anti-stacking mode were considered. First, we assumed that all stacking distances between consecutive monomers are equal, that is, there is no stacking distance alternation, so that covalent-like intermolecular interaction effects are expected to extend over the whole aggregate. Figure 5a shows the variation of the  $y_0$  and  $y_1$  diradical characters as a function of  $d$  for the tetramer (see also Table S3 in the Supporting Information). Owing to the nonzero

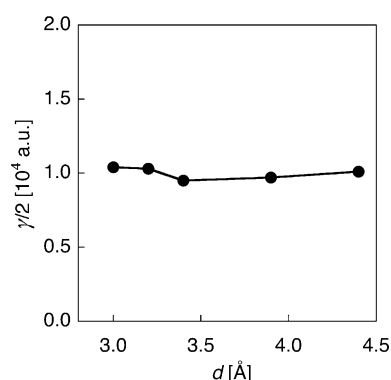


**Figure 4.** Values of  $\gamma/2$  calculated using the LC-RBLYP/6-31+G\* method as a function of stacking distance  $d$  for coronene dimers.

values of  $y_0$  and  $y_1$  together with negligible  $y_i$  ( $i \geq 2$ ), the phenalenyl tetramers are regarded as tetraradical systems. As in the case of dimers,  $y$  varies as a function of increasing  $d$  from small, near 0, values to large values close to 1. For instance, the tetramer with  $d = 2.8$  Å displays  $y_0 = 0.296$  and  $y_1 = 0.061$ , whereas for  $d = 4.4$  Å both  $y_0$  and  $y_1$  are close to 1 ( $y_0 = 0.950$  and  $y_1 = 0.869$ ).

Figure 5b shows that  $\gamma/4$  versus  $d$  for the tetramer also exhibits an enhancement at intermediate  $y$  values. For  $d = 3.0$  Å, which corresponds to an intermediate tetraradical character ( $y_0 = 0.511$  and  $y_1 = 0.159$ ),  $\gamma/4 = 40.5 \times 10^4$  a.u. is more than 130 times as large as for the isolated monomer, and larger than in the case of the dimer (30 times). These results highlight a remarkable multiradical effect on the NLO property in open-shell aggregates. Figure 6a,d display  $D^{\text{odd}}(r)$  and  $\rho^{(3)}(r)$  for the

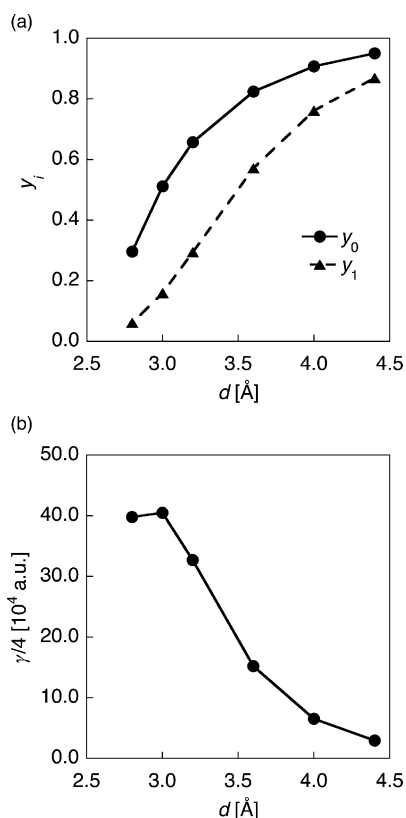


**Figure 5.** a) Diradical characters ( $y_0$  and  $y_1$ ) and b)  $\gamma/4$  values calculated using the LC-UBLYP/6-31+G\* method as a function of stacking distance  $d$  for anti-type phenalenyl tetramers.

phenalenyl tetramer with  $d=3.2$  Å, respectively. Though  $D^{\text{odd}}(r)$  is similar to the dimer case and almost evenly distributed on the four monomers—with slightly larger amplitudes on the external ones— $\rho^{(3)}(r)$  is exalted and localized on the external monomers.

The alternation of the stacking distances is expected to impact the  $y$  and  $\gamma$  value, as evidenced by studies on model one-dimensional hydrogen chains and hydrogen clusters.<sup>[9]</sup> In that case, the alternation (an alignment of stacking distances  $(d_1, d_2)_n$  in which  $d_1$  (to give intermediate  $y_0$ )  $<$   $d_2$ ) leads to a decrease in  $y_0$  and an increase in  $y_1$ , which reduces the  $\gamma$  enhancement in the intermediate open-shell character region and decreases the size-dependent evolution of  $\gamma$ . These alternation effects have been confirmed for the phenalenyl aggregates by performing additional calculations on a neutral tetramer in anti conformation. For an alternating tetramer characterized by  $(d_1, d_2)=(3.0 \text{ Å}, 3.5 \text{ Å})$ ,  $(y_0, y_1)=(0.384, 0.229)$  and  $\gamma/\text{monomer}=28.5 \times 10^4$  a.u., which should be compared to the  $(y_0, y_1)=(0.511, 0.159)$  and  $\gamma/\text{monomer}=40.5 \times 10^4$  a.u. for the non-alternating model with  $(d_1, d_2)=(3.0 \text{ Å}, 3.0 \text{ Å})$ . Further analysis is provided in Figures S2 and S3 of the Supporting Information.

### Spin and charge effects

Finally, the spin and charge state effects in these open-shell aggregates were studied. Table 2 lists the diradical characters ( $y_0$  and  $y_1$ ) and  $\gamma$  values for the phenalenyl tetramer for a stacking distance of 3.2 Å in its neutral singlet, neutral quintet (the highest spin state for a tetradical), and dicationic singlet

**Table 2.** Diradical characters ( $y_0$  and  $y_1$ ) and  $\gamma$  values for the anti-phenalenyl tetramer at stacking distance  $d=3.2$  Å in the neutral singlet, neutral quintet, and dicationic singlet states calculated using the LC-UBLYP/6-31+G\* method.

State	$y_0$	$y_1$	$\gamma$ [ $10^4$ a.u.]
neutral singlet	0.657	0.294	131
neutral quintet	–	–	2.94
dicationic singlet	0.597	0.012	1730

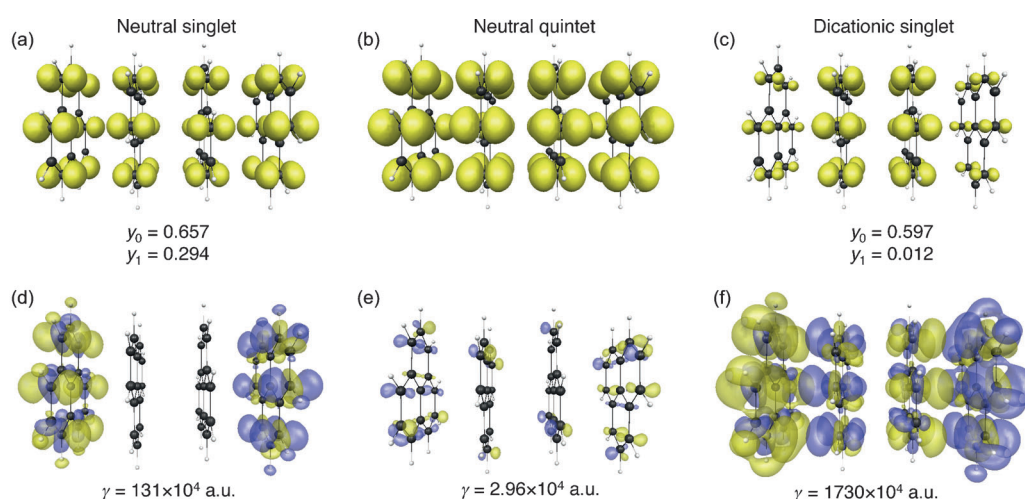


**Figure 6.** Odd-electron density distributions for the anti-phenalenyl tetramer with  $d=3.2$  Å in the a) neutral singlet, b) neutral quintet, and c) dicationic singlet states as well as their  $y_0$  and  $y_1$  values in which the isosurfaces of 0.002 a.u. are shown. d–f) The  $\gamma$  density distributions and  $\gamma$  values for the same systems are also shown. The yellow and blue meshes represent positive and negative distributions with isosurfaces of  $\pm 1200$  a.u. for the neutral singlet tetramer, of  $\pm 30$  a.u. for the neutral quintet one, and of  $\pm 10000$  a.u. for the dicationic singlet one.

states. It is generally predicted that open-shell singlet systems with intermediate  $\gamma$  exhibit a significant reduction of  $\gamma$  by going to the highest spin state because the overlaps between the radicals vanish owing to Pauli repulsion.<sup>[2b,4a,c]</sup> As with typical open-shell molecules investigated in previous studies,  $\gamma$  of the tetramer decreases remarkably by switching from the singlet ( $131 \times 10^4$  a.u.) to the quintet state ( $2.96 \times 10^4$  a.u.), whereby the  $\gamma(\text{singlet})/\gamma(\text{quintet})$  ratio attains 44. In a concomitant way, the  $D^{\text{odd}}(r)$  distributions change and get larger and similar for each monomer. This indicates that the commutation from the singlet to the quintet state consists simply of spin flips of radical electrons from antiparallel to parallel, which then break the weak intermolecular covalent bonds and lead to an enhancement of the  $D^{\text{odd}}(r)$  amplitudes. The negligibly small  $\rho^{(3)}(r)$  amplitude exemplifies the significant  $\gamma$  reduction.

However, by going to the dicationic singlet state,  $\gamma$  is enhanced by more than one order of magnitude with respect to the neutral state ( $131 \times 10^4$  a.u.  $\rightarrow$   $1730 \times 10^4$  a.u.). The intermediate  $\gamma_0$  (0.597) and negligible  $\gamma_1$  (0.012) values imply that the tetramer has switched from an intermediate tetradical to an intermediate diradical system upon double ionization. Additionally, the  $D^{\text{odd}}(r)$  distribution for the dication, shown in Figure 6c, is primarily distributed on the internal two units. These changes in  $\gamma$  and  $D^{\text{odd}}(r)$  from the neutral to the dicationic state illustrate that the two odd electrons localized on the terminal phenalenyl units in the neutral state are removed in the dicationic state. This feature is supported by the distribution of the electronic density difference between the neutral and dicationic states,  $\rho(\text{neutral}) - \rho(\text{dicationic})$ , which are mostly localized on the terminal units (see Figure 7). Consequently, the electronic structure of the dicationic tetramer exhibits an intermediate diradical nature, mostly in the inner phenalenyl molecules surrounded by cationic phenalenyls, and it corresponds to a kind of acceptor- $\pi$ -acceptor system. This acceptor- $\pi$ -acceptor pattern can explain the substantial  $\gamma$  enhancement by means of through-space conjugation.<sup>[24]</sup> Recently, such a charge-transfer effect is also predicted to further enhance the  $\gamma$  values for open-shell singlet systems.<sup>[25]</sup> The value of  $\rho^{(3)}(r)$  (see Figure 6f) displays large amplitudes over the four

units with alternating positive and negative signs. This indicates that hole sites on the cations boost the field-induced odd-electrons variations and field-induced intermolecular charge transfers.

## Conclusion

In this study, the impact of intermolecular interactions on the open-shell characters  $\gamma$  and second hyperpolarizabilities  $\gamma$  of open-shell 1D molecular aggregates composed of  $\pi$ - $\pi$  stacked phenalenyl radicals has been revealed by using first-principles calculations. In the singlet states the phenalenyl dimers cover the whole range of diradical character, from nearly closed-shell to pure diradical, depending on the intermolecular stacking distance. In particular, the phenalenyl dimer with a stacking distance close to the experimental one exhibits an intermediate  $\gamma$  value, which indicates covalent-like intermolecular interactions. The dimerization of phenalenyl radicals leads to giant enhancements of  $\gamma$ , which strongly depend on  $\gamma$  following the structure-property relationships observed in diradical molecules. In particular, the  $\gamma$  per monomer can show up to a 30-fold enhancement relative to the isolated monomer, provided  $\gamma$  is intermediate. However, this  $\gamma$  enhancement due to dimerization is not observed in the coronene dimer, which is regarded as the corresponding closed-shell prototype. Then, again for intermediate  $\gamma$  characters, the phenalenyl tetramers exhibit larger  $\gamma$  enhancements, which can attain a factor of 130. Furthermore, significant spin- and charge-state dependences of  $\gamma$  are observed in these open-shell aggregates. For the intermediate tetradical phenalenyl tetramer, changing from the singlet to the quintet state significantly reduces  $\gamma$  (by a factor of 44), whereas the  $\gamma$  of the dication is more than 10 times as large as that of the neutral one. On the basis of these results, it is concluded that open-shell molecules that form aggregates and are subsequently in the solid state are expected to display remarkable changes in their electronic structure (i.e., multiradical character) owing to covalent-like intermolecular interactions, which are not observed in closed-shell aggregates, and that gigantic  $\gamma$  enhancement outstrips the conventional control and design scheme of the NLO properties based on tuning the chemical structure of single molecules. This study demonstrates the immense potential of open-shell molecular aggregates with a wide variety of multiradical structures as well as of charge and spin states in the realization of a novel class of highly efficient NLO materials.

## Acknowledgements

This work was supported by a Grant-in-Aid for Bilateral Programs Joint Research Projects (JSPS, F.R.S.-FNRS), a Grant-in-Aid for Scientific Research (A) (no. 25248007) from the Japan Society for the Promotion of Science (JSPS), a Grant-in-Aid for Scientific Research on Innovative Areas (no. A24109002a), MEXT, the Strategic Programs for Innovative Research (SPIRE), MEXT, and the Computational Materials Science Initiative (CMSI), Japan. It is also supported by the Academy Louvain (ARC "Ex-

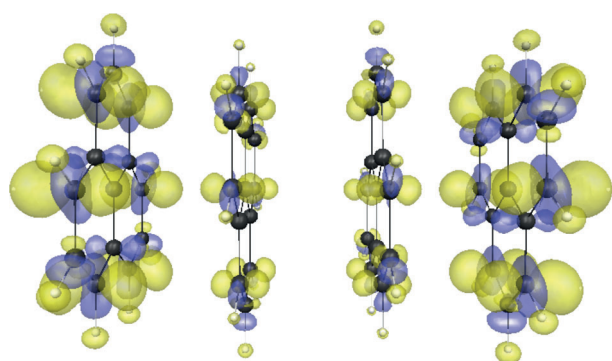


**Figure 7.** Distribution of the electron density difference for anti-phenalenyl tetramers with a stacking distance  $d = 3.2$  Å in the neutral and dicationic states ( $\rho(\text{neutral}) - \rho(\text{dicationic})$ ). The yellow and blue meshes represent positive and negative electron distributions with isosurfaces of  $\pm 0.002$  a.u., respectively.



tended  $\pi$ -Conjugated Molecular Tinkertoys for Optoelectronics, and Spintronics”) and by the Belgian Government (IUAP no. P07-12 “Functional Supramolecular Systems”).

**Keywords:** aggregation • density functional calculations • nonlinear optics • pi interactions • radicals

- [1] a) S. Tao, T. Miyagoe, A. Maeda, H. Matsuzaki, H. Ohtsu, M. Hasegawa, S. Takaishi, M. Yamashita, H. Okamoto, *Adv. Mater.* **2007**, *19*, 2707–2710; b) D. A. Parthenopoulos, P. M. Rentzepis, *Science* **1989**, *245*, 843–845; c) W. Zhou, S. M. Kuebler, K. L. Braun, T. Yu, J. K. Cammack, C. K. Ober, J. W. Perry, S. R. Marder, *Science* **2002**, *296*, 1106–1109; d) S. Kawata, Y. Kawata, *Chem. Rev.* **2000**, *100*, 1777–1788; e) J. Wang, Y. Chen, W. J. Blau, *J. Mater. Chem.* **2009**, *19*, 7425–7443; f) P. K. Frederiksen, M. Jørgensen, P. R. Ogilby, *J. Am. Chem. Soc.* **2001**, *123*, 1215–1221.
- [2] a) M. Nakano, R. Kishi, T. Nitta, T. Kubo, K. Nakasuji, K. Kamada, K. Ohta, B. Champagne, E. Botek, K. Yamaguchi, *J. Phys. Chem. A* **2005**, *109*, 885–891; b) M. Nakano, R. Kishi, N. Nakagawa, S. Ohta, H. Takahashi, S. Furukawa, K. Kamada, K. Ohta, B. Champagne, E. Botek, S. Yamada, K. Yamaguchi, *J. Phys. Chem. A* **2006**, *110*, 4238–4243; c) M. Nakano, R. Kishi, S. Ohta, A. Takebe, H. Takahashi, S. Furukawa, T. Kubo, Y. Morita, K. Nakasuji, K. Yamaguchi, K. Kamada, K. Ohta, B. Champagne, E. Botek, *J. Chem. Phys.* **2006**, *125*, 074113; d) M. Nakano, T. Kubo, K. Kamada, K. Ohta, R. Kishi, S. Ohta, N. Nakagawa, H. Takahashi, S. Furukawa, Y. Morita, K. Nakasuji, K. Yamaguchi, *Chem. Phys. Lett.* **2006**, *418*, 142–147; e) R. Kishi, M. Dennis, K. Fukuda, Y. Murata, K. Morita, H. Uenaka, M. Nakano, *J. Phys. Chem. C* **2013**, *117*, 21498–21508.
- [3] a) E. F. Hayes, A. K. Q. Siu, *J. Am. Chem. Soc.* **1971**, *93*, 2090–2091; b) K. Yamaguchi in *Self-Consistent Field: Theory and Applications*, (Eds.: R. Carbo, M. Klobukowski), Elsevier, Amsterdam, **1990**, pp. 727–828; c) K. Kamada, K. Ohta, A. Shimizu, T. Kubo, R. Kishi, H. Takahashi, E. Botek, B. Champagne, M. Nakano, *J. Phys. Chem. Lett.* **2010**, *1*, 937–940; d) M. Head-Gordon, *Chem. Phys. Lett.* **2003**, *372*, 508–511.
- [4] a) M. Nakano, H. Nagai, H. Fukui, K. Yoneda, R. Kishi, H. Takahashi, A. Shimizu, T. Kubo, K. Kamada, K. Ohta, B. Champagne, E. Botek, *Chem. Phys. Lett.* **2008**, *467*, 120–125; b) H. Nagai, M. Nakano, K. Yoneda, R. Kishi, H. Takahashi, A. Shimizu, T. Kubo, K. Kamada, K. Ohta, E. Botek, B. Champagne, *Chem. Phys. Lett.* **2010**, *489*, 212–218; c) K. Yoneda, M. Nakano, H. Fukui, T. Minami, Y. Shigeta, T. Kubo, K. Ohta, E. Botek, B. Champagne, *ChemPhysChem* **2011**, *12*, 1697–1707; d) K. Yoneda, M. Nakano, Y. Inoue, T. Inui, K. Fukuda, Y. Shigeta, T. Kubo, B. Champagne, *J. Phys. Chem. C* **2012**, *116*, 17787–17795; e) K. Yoneda, M. Nakano, K. Fukuda, B. Champagne, *J. Phys. Chem. Lett.* **2012**, *3*, 3338–3342.
- [5] a) H. Fukui, M. Nakano, Y. Shigeta, B. Champagne, *J. Phys. Chem. Lett.* **2011**, *2*, 2063–2066; b) H. Fukui, M. Nakano, B. Champagne, *Chem. Phys. Lett.* **2012**, *527*, 11–15; c) H. Fukui, Y. Inoue, T. Yamada, S. Ito, Y. Shigeta, R. Kishi, B. Champagne, M. Nakano, *J. Phys. Chem. A* **2012**, *116*, 5501–5509.
- [6] a) M. Nakano, R. Kishi, S. Ohta, H. Takahashi, T. Kubo, K. Kamada, K. Ohta, E. Botek, B. Champagne, *Phys. Rev. Lett.* **2007**, *99*, 033001; b) M. Nakano, K. Yoneda, R. Kishi, H. Takahashi, T. Kubo, K. Kamada, K. Ohta, E. Botek, B. Champagne, *J. Chem. Phys.* **2009**, *131*, 114316; c) M. Nakano, B. Champagne, E. Botek, K. Ohta, K. Kamada, T. Kubo, *J. Chem. Phys.* **2010**, *133*, 154302; d) M. Nakano, B. Champagne, *J. Chem. Phys.* **2013**, *138*, 244306.
- [7] a) T. Kubo, A. Shimizu, M. Sakamono, M. Uruichi, K. Yakushi, M. Nakano, D. Shiomi, K. Sato, T. Takui, Y. Morita, K. Nakasuji, *Angew. Chem.* **2005**, *117*, 6722–6726; *Angew. Chem. Int. Ed.* **2005**, *44*, 6564–6568; b) T. Kubo, A. Shimizu, M. Uruichi, K. Yakushi, M. Nakano, D. Shiomi, K. Sato, T. Takui, Y. Morita, K. Nakasuji, *Org. Lett.* **2007**, *9*, 81–84.
- [8] K. Kamada, K. Ohta, T. Kubo, A. Shimizu, Y. Morita, K. Nakasuji, R. Kishi, S. Ohta, S. Furukawa, H. Takahashi, M. Nakano, *Angew. Chem.* **2007**, *119*, 3614–3616; *Angew. Chem. Int. Ed.* **2007**, *46*, 3544–3546.
- [9] a) M. Nakano, A. Takebe, R. Kishi, S. Ohta, M. Nate, T. Kubo, K. Kamada, K. Ohta, B. Champagne, E. Botek, H. Takahashi, S. Furukawa, Y. Morita, K. Nakasuji, *Chem. Phys. Lett.* **2006**, *432*, 473–479; b) M. Nakano, T. Minami, H. Fukui, R. Kishi, Y. Shigeta, B. Champagne, *J. Chem. Phys.* **2012**, *136*, 024315 (1–7).
- [10] M. Nakano, A. Takebe, R. Kishi, H. Fukui, T. Minami, K. Kubota, H. Takahashi, T. Kubo, K. Kamada, K. Ohta, B. Champagne, E. Botek, *Chem. Phys. Lett.* **2008**, *454*, 97–104.
- [11] K. Goto, T. Kubo, K. Yamamoto, K. Nakasuji, K. Sato, D. Shiomi, T. Takui, M. Kubota, T. Kobayashi, K. Yakushi, J. Ouyang, *J. Am. Chem. Soc.* **1999**, *121*, 1619–1620.
- [12] a) J. Huang, M. Kertesz, *J. Phys. Chem. A* **2007**, *111*, 6304–6315; b) B. Kolb, M. Kertesz, T. Thonhauser, *J. Phys. Chem. A* **2013**, *117*, 3642–3649; c) Y.-H. Tian, M. Kertesz, *J. Am. Chem. Soc.* **2010**, *132*, 10648–10649.
- [13] R.-L. Zhong, H.-L. Xu, S.-L. Sun, Y.-Q. Qiu, L. Zhao, Z.-M. Su, *J. Chem. Phys.* **2013**, *139*, 124314 (1–6).
- [14] a) H. Stoll and A. Savin in *Density Functional Methods in Physics*, (Eds.: R. Dreizler, J. da Providencia), Plenum, New York **1985**, pp. 177–207; b) H. Iikura, T. Tsuneda, T. Yanai, K. Hirao, *J. Chem. Phys.* **2001**, *115*, 3540–3544.
- [15] S. Grimme, *J. Comput. Chem.* **2006**, *27*, 1787–1799.
- [16] S. F. Boys, F. Bernardi, *Mol. Phys.* **1970**, *19*, 553–566.
- [17] a) C. Lambert, *Angew. Chem.* **2011**, *123*, 1794–1796; *Angew. Chem. Int. Ed.* **2011**, *50*, 1756–1758; b) M. Abe, *Chem. Rev.* **2013**, *113*, 7011–7088.
- [18] M. Nakano, H. Fukui, T. Minami, K. Yoneda, Y. Shigeta, R. Kishi, B. Champagne, E. Botek, T. Kubo, K. Ohta, K. Kamada, *Theor. Chem. Acc.* **2011**, *130*, 711–724; erratum *130*, 725–726.
- [19] a) R. Kishi, S. Bonness, K. Yonda, H. Takahashi, M. Nakano, E. Botek, B. Champagne, T. Kubo, K. Kamada, K. Ohta, T. Tsuneda, *J. Chem. Phys.* **2010**, *132*, 094107; b) S. Bonness, H. Fukui, K. Yoneda, R. Kishi, B. Champagne, E. Botek, M. Nakano, *Chem. Phys. Lett.* **2010**, *493*, 195–199.
- [20] H. D. Cohen, C. C. J. Roothaan, *J. Chem. Phys.* **1965**, *43*, S34–S39.
- [21] M. Nakano, I. Shigemoto, S. Yamada, K. Yamaguchi, *J. Chem. Phys.* **1995**, *103*, 4175–4191.
- [22] *Gaussian 09, Revision B.01*, M. J. Frisch, G. W. Trucks, H. B. Schlegel, G. E. Scuseria, M. A. Robb, J. R. Cheeseman, G. Scalmani, V. Barone, B. Menucci, G. A. Petersson, H. Nakatsuji, M. Caricato, X. Li, H. P. Hratchian, A. F. Izmaylov, J. Bloino, G. Zheng, J. L. Sonnenberg, M. Hada, M. Ehara, K. Toyota, R. Fukuda, J. Hasegawa, M. Ishida, T. Nakajima, Y. Honda, O. Kitao, H. Nakai, T. Vreven, J. A. Montgomery, Jr., J. E. Peralta, F. Ogliaro, M. Bearpark, J. J. Heyd, E. Brothers, K. N. Kudin, V. N. Staroverov, R. Kobayashi, J. Normand, K. Raghavachari, A. Rendell, J. C. Burant, S. S. Iyengar, J. Tomasi, M. Cossi, N. Rega, N. J. Millam, M. Klene, J. E. Knox, J. B. Cross, V. Bakken, C. Adamo, J. Jaramillo, R. Gomperts, R. E. Stratmann, O. Yazyev, A. J. Austin, R. Cammi, C. Pomelli, J. W. Ochterski, R. L. Martin, K. Morokuma, V. G. Zakrzewski, G. A. Voth, P. Salvador, J. J. Dannenberg, S. Dapprich, A. D. Daniels, Ö. Farkas, J. B. Foresman, J. V. Ortiz, J. Cioslowski, D. J. Fox, Gaussian, Inc., Wallingford CT, USA, **2009**.
- [23] a) J.-M. Lü, S. V. Rosokha, J. K. Kochi, *J. Am. Chem. Soc.* **2003**, *125*, 12161–12171; b) S. Suzuki, Y. Morita, K. Fukui, K. Sato, D. Shiomi, T. Takui, K. Nakasuji, *J. Am. Chem. Soc.* **2006**, *128*, 2530–2531.
- [24] O. Xie, C. W. Dirk, *J. Phys. Chem. B* **1998**, *102*, 9378–9384.
- [25] K. Fukuda, M. Nakano, *J. Phys. Chem. A* **2014**, *118*, 3463–3471.

Received: February 15, 2014

Published online on July 23, 2014